Molecular Cell
Article

CellPress

A Synthetic Multifunctional Mammalian pH Sensor and CO_2 Transgene-Control Device

David Ausländer,[1] Simon Ausländer,[1] Ghislaine Charpin-El Hamri,[2] Ferdinand Sedlmayer,[1] Marius Müller,[1] Olivier Frey,[1] Andreas Hierlemann,[1] Jörg Stelling,[1] and Martin Fussenegger[1,*]
[1]Department of Biosystems Science and Engineering, ETH Zurich, Mattenstrasse 26, 4058 Basel, Switzerland
[2]IUT Lyon 1, Département Génie Biologique, 74 Boulevard Niels Bohr, 69622 Villeurbanne Cedex, France
*Correspondence: fussenegger@bsse.ethz.ch
http://dx.doi.org/10.1016/j.molcel.2014.06.007

SUMMARY

All metabolic activities operate within a narrow pH range that is controlled by the CO_2-bicarbonate buffering system. We hypothesized that pH could serve as surrogate signal to monitor and respond to the physiological state. By functionally rewiring the human proton-activated cell-surface receptor TDAG8 to chimeric promoters, we created a synthetic signaling cascade that precisely monitors extracellular pH within the physiological range. The synthetic pH sensor could be adjusted by organic acids as well as gaseous CO_2 that shifts the CO_2-bicarbonate balance toward hydrogen ions. This enabled the design of gas-programmable logic gates, provided remote control of cellular behavior inside microfluidic devices, and allowed for CO_2-triggered production of biopharmaceuticals in standard bioreactors. When implanting cells containing the synthetic pH sensor linked to production of insulin into type 1 diabetic mice developing diabetic ketoacidosis, the prosthetic network automatically scored acidic pH and coordinated an insulin expression response that corrected ketoacidosis.

INTRODUCTION

Synthetic biology is the science of reassembling cataloged and standardized biological items in a systematic and rational manner to create and engineer biological designer devices, systems, and organisms with novel and useful functions (Khalil and Collins, 2010; Marguet et al., 2007; Weber and Fussenegger, 2012). During the past decade, mammalian synthetic biology has progressed from simple control switches providing trigger-inducible transgene expression to complex transcription/translation networks enabling oscillating expression dynamics (Tigges et al., 2009), intercellular communication (Bacchus et al., 2012), and fundamental arithmetic operations (Ausländer et al., 2012). To date, synthetic biology-inspired biomedical applications have been successfully tested in animal models including T cell therapy (Chen et al., 2010), treatment of gouty arthritis (Kemmer et al., 2010), obesity (Rössger et al., 2013b), and type 2 diabetes (Ye et al., 2011).

Type 1 diabetes mellitus is a chronic metabolic disease that is characterized by excessive blood glucose levels resulting from autoimmune destruction of insulin-producing β cells in the islets of Langerhans of the pancreas (Pozzilli, 2012). The lack of insulin dramatically decreases the insulin-dependent glucose transporter (GLUT-4)-mediated glucose uptake in muscle and adipose tissues, which leads to uncontrolled lipolysis in adipose tissue and ultimately increased production of ketone bodies in the liver. Unless counteracted by insulin, which switches from fat- to glucose-based energy supplies, excess acidic ketone bodies accumulate in the blood, overwhelm the acid-base homeostasis maintained by the CO_2-bicarbonate buffering system, and produce medical conditions ranging from mild acidosis ($pH < 7.35$) to acute diabetic ketoacidosis (DKA; $pH < 7.1$) leading to cerebral edema, coma, and death (Kitabchi et al., 2001). Since there is no cure available yet, current treatment strategies include lifelong insulin replacement therapy by subcutaneous injection or insulin pumps along with precise dietary management and careful monitoring of blood glucose levels (Pickup, 2012). This requires training, appropriate care, and discipline in testing and dosing, which is particularly challenging for children, adolescents, disabled and elderly patients, and during intercurrent infection-related disturbances of insulin levels. Although pancreas and islet cell transplantation have also been successfully established, these therapies are considered dangerous, require a lot of donor material, and essentially replace lifelong insulin therapy by lifelong treatment with immunosuppressive agents; associated risks include severe infections and cancer (Larsen, 2004). Poorly managed glucose homeostasis may result in a variety of complications including cardiovascular disease, diabetic neuropathy, and diabetic retinopathy, as well as DKA (Hovorka, 2011).

Since life operates in aqueous solutions, it is no surprise that pH is a key parameter that impacts protein folding, stability, protein-protein interactions, and activity and therefore needs to be reliably kept within a narrow biochemically permissive range (e.g., pH 7.35–7.45 in humans) (Casey et al., 2010). The CO_2-bicarbonate buffering system manages acid-base homeostasis and maintains almost constant pH in all living systems, including humans. In a reversible reaction catalyzed by carbonic anhydrases, gaseous CO_2 reacts with H_2O to form carbonic acid, which rapidly dissociates into bicarbonate and hydrogen ions. Increases in CO_2 resulting from oxidative metabolism are

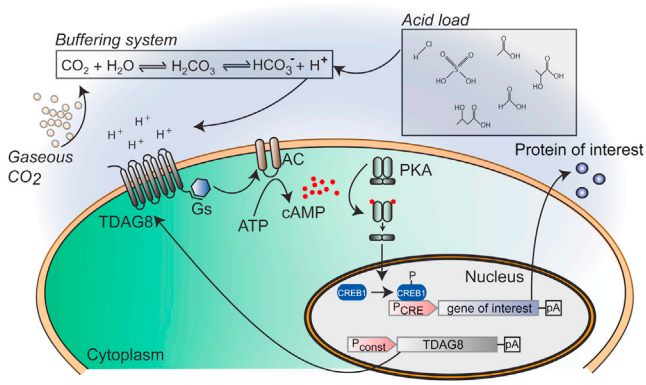

Figure 1. Design of the Synthetic pH-Sensor Device

The constitutively expressed G protein-coupled receptor TDAG8 senses extracellular proton levels and triggers, via a specific G protein (G_s), pH-adjusted activation of the membrane-bound adenylyl cyclase (AC) that converts ATP into the second messenger cyclic AMP (cAMP). When rewiring the resulting intracellular cAMP surge to cAMP-mediated activation of PKA's (protein kinase A's) regulatory subunits, the cAMP-dependent phosphokinase releases its catalytic subunits, which translocate into the nucleus where they phosphorylate and actuate the cAMP-responsive element-binding protein 1 (CREB1). Activated CREB1 binds to synthetic promoters (P_{CRE}) containing cAMP-response elements (CRE) and induces P_{CRE}-driven transgenes in response to pH changes resulting either from shifts in the CO_2-bicarbonate buffering system induced by gaseous carbon dioxide (CO_2) or by addition of (in)organic acids.

balanced by elimination of gaseous CO_2 through alveolar ventilation. Because of the strict correlation between H^+ and CO_2 in aqueous solutions, CO_2 can shift this balance toward high proton concentration and so critically influences culture, tissue, and body pH (Tresguerres et al., 2010). Therefore, gaseous CO_2 is also used to control pH in cell culture systems and biopharmaceutical manufacturing in a traceless and noninvasive manner (Wurm, 2004).

Specialized human cells express a variety of extracellular and intracellular acid-sensing proteins that monitor pH and adapt physiological activities to pH changes. For example, members of the acid-sensing ion channels (ASICs) expressed in primary sensory neurons modulate pain (Waldmann et al., 1997), and transient receptor potential (TRP) ion channels function as sour taste receptors (Tominaga et al., 1998). In addition, a group of G protein-coupled receptors (GPCRs) such as ovarian cancer G protein-coupled receptor 1 (OGR1), GPR4, and T cell death-associated gene 8 (TDAG8) monitors pH via histidine residues in their extracellular domain, but the proteins' physiological functions are not yet clearly established (Ishii et al., 2005; Ludwig et al., 2003). Since TDAG8 transcripts have been identified predominantly in nerve and immune cells, the receptor has been suggested to modulate pain reactions and immune responses. Here, we hypothesized that proton-sensing GPCRs could be used to monitor physiological functions via the surrogate signal pH, and that synthetic devices could be designed to act upon perturbed physiological states such as DKA. Capitalizing on ectopic expression of TDAG8, we assembled a designer cascade that was able to precisely sense culture pH (pH-Sensor), program Boolean expression logic, and trigger transgene expression in mammalian cells grown in culture, inside microfluidic devices and state-of-the-art bioreactors by gaseous CO_2 (CO_2ntrol). We also developed a prosthetic gene network that corrects DKA and restores glucose homeostasis in mice suffering from type 1 diabetes (pH-Guard). Synthetic pH-Sensor, CO_2ntrol, and pH-Guard may significantly advance gene function analysis, the production of difficult-to-express protein therapeutics, and gene and cell-based therapies.

RESULTS

Design and Validation of a Synthetic Mammalian pH-Sensor

Although the precise physiological function of the G protein-coupled receptor TDAG8 remains elusive, it has been shown to sense extracellular protons and trigger a heterotrimeric G_s-protein response that leads to activation of the adenylate cyclase and results in an intracellular cyclic AMP (cAMP) surge (Ishii et al., 2005). By functionally linking cAMP levels to activation of the protein kinase A (PKA), phosphorylation of the cAMP-responsive element-binding protein 1 (CREB1), and CREB1-mediated induction of synthetic P_{CRE} promoters, extracellular pH could be directly rewired to desired transgene expression (Figure 1). We cotransfected TDAG8 expression units driven by different constitutive promoters ($P_{hEF1\alpha}$/P_{hCMV}/P_{SV40}-TDAG8-pA; pDA55/pDA33/pDA62) with P_{CRE}-driven SEAP (P_{CRE}-SEAP-pA, pCK53) or EYFP (P_{CRE}-EYFP-pA, pCK91) expression vectors into different mammalian cell lines. Reporter gene expression in human embryonic kidney cells (HEK293), a HEK293-derived production cell line adapted for growth in protein-free suspension cultures (FreeStyle 293-F), Chinese hamster ovary cells (CHO-K1), and human mesenchymal stem cells (hMSC-TERT), could be reliably switched ON and OFF in all cell lines by corresponding low and high pH within the human physiological range (pH6.9 and pH7.6) (Figure 2A). As expected, possible differences in the availability and compatibility of the promiscuous TDAG8-compatible G proteins and the efficiency of the intrinsic cAMP signaling pathway may in part explain differences in basal expression and induction profiles among different cell lines (Rössger et al., 2013a). Control experiments showed (1) that pTDAG8 neither reduced cell viability (Figures S1A and S1B) nor maximum SEAP production levels over the entire pH range (Figure 2B); (2) that the culture pH could be precisely adjusted and remained constant during expression profiling (Figure S1C); (3) that P_{CRE}-driven SEAP and EYFP production was repressed in the absence of TDAG8 expression within the entire physiological pH range (Figure 2B; Figure S2); (4) that pH-triggered expression switches correlated with cAMP levels (Figure S1D); (5) that the TDAG8-to-P_{CRE} signaling could be interrupted by the PKA inhibitor H-89, confirming the exclusive rewiring (Figure S1E); and (6) that physiological concentrations of ligands targeting HEK293's endogenous GPCRs that also influence the cAMP-dependent pathway did not interfere with signaling (Figure S1F).

The pH-Sensor device was shut down within the normal physiologic pH range of the human body (pH7.35–7.45) and was gradually induced at a lower pH (pH 7.35–6.5) that correlated with DKA (Barker et al., 2004) (Figure 2B; EC_{50} = pH

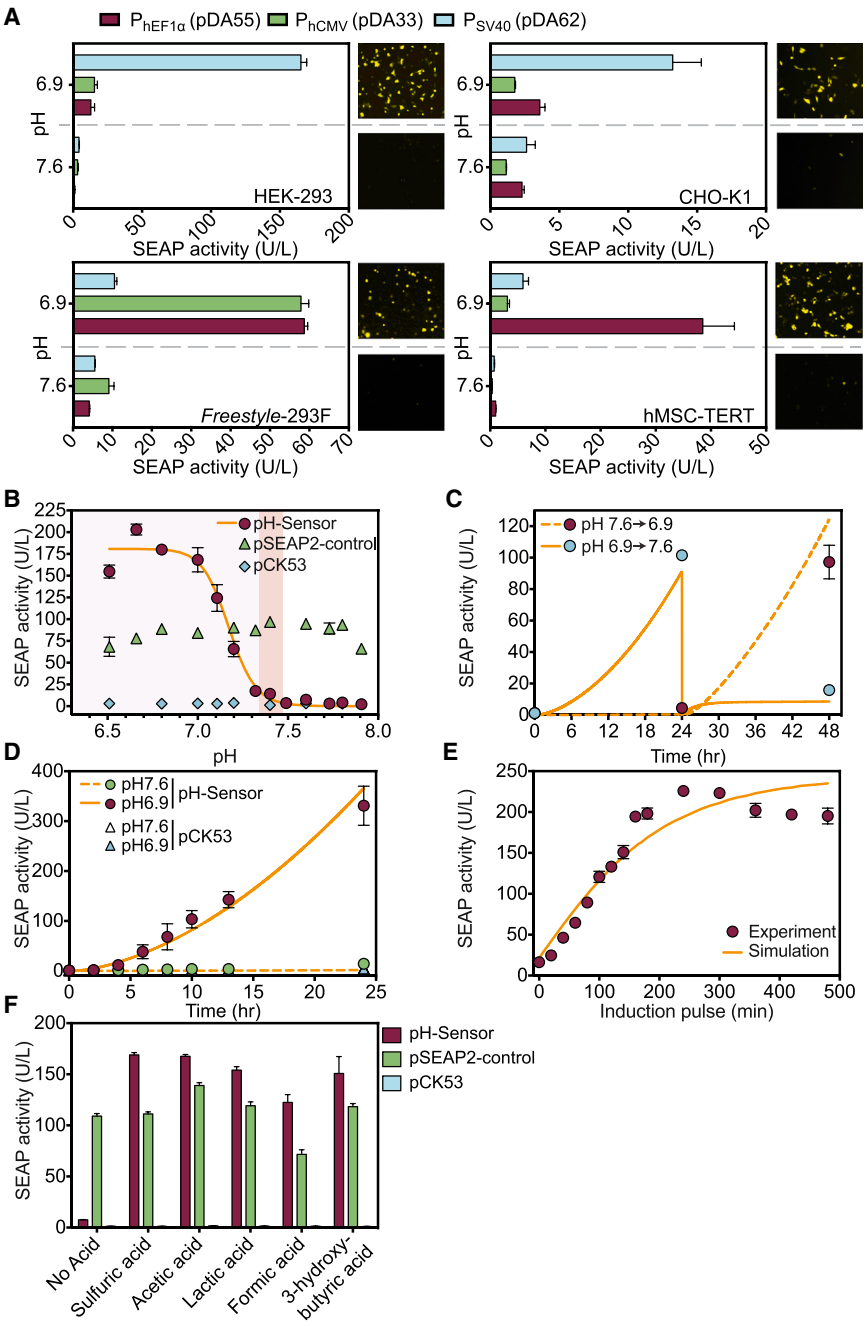

Figure 2. Characterization of the pH-Sensor

(A) pH-Sensor performance in different mammalian cell lines. Indicated cell lines were cotransfected with a constitutive TDAG8 expression vector ($P_{hEF1\alpha}$/P_{hCMV}/P_{SV40}-TDAG8-pA; pDA55/pDA33/pDA62) as well as a P_{CRE}-driven SEAP expression plasmid (pCK53, P_{CRE}-SEAP-pA) and exposed to high (7.6) or low (6.9) physiologic pH for 24 hr before SEAP expression was quantified in the culture supernatant. Likewise, the best-in-class TDAG8 expression vector of each cell line (pDA62, HEK293/CHO-K1; pDA55, FreeStyle 293F/hMSC-TERT) was cotransfected with a P_{CRE}-driven EYFP expression, and reporter gene expression was visualized by fluorescence microscopy after a 24 hr cultivation period at high and low pH.

(B) Sensitivity and adjustability of the pH-Sensor. HEK293 cells were (co)transfected with pH-Sensor-encoding vectors (pDA62/pCK53), a constitutive SEAP expression plasmid (pSEAP2-control), or the P_{CRE}-driven SEAP reporter construct (pCK53) and cultivated for 24 hr in medium adjusted to different pH values before SEAP was profiled in the culture supernatant. Red translucent background represents the narrow range of human blood pH (pH 7.35–7.45) while the gray transparent background indicates pH values associated with human acidosis (pH < 7.35). EC_{50} = pH 7.15 ± 0.03.

(C) Reversibility of the pH-Sensor. The reversibility of pH-Sensor-driven SEAP expression was assessed by cultivating engineered HEK293 cells for 48 hr in medium adjusted to high (7.6) or low (6.9) pH while resetting the cell density to 1 × 10^5 cells/ml and alternating the culture pH after 24 hr.

(D) pH-Sensor induction kinetics. pH-Sensor-engineered HEK293 cells were grown in medium adjusted to high (7.6) or low (6.9) pH, and SEAP expression was profiled for 24 hr.

(E) Programming pH-Sensor induction kinetics. SEAP expression profiles of HEK293 cells (co)transfected with pH-Sensor components that were exposed to different induction pulses with low-pH (6.9) culture medium.

(F) Sensitivity of the pH-Sensor to different acid loads. HEK293 cells (co)transfected with pH-Sensor components, pSEAP2-control, or the P_{CRE}-driven SEAP reporter vector alone were cultivated for 24 hr in medium acidified to pH 6.9 using different (in)organic acids before SEAP expression was assessed in the cell culture supernatant. Orange curves show corresponding model-based simulations. Data presented are mean ± SEM, n ≥ 3. See also Figures S1–S5.

7.15 ± 0.03). The pH-dependent transgene expression switches were reversible (Figure 2C), showed rapid induction kinetics with robust expression levels (Figure 2D; Figure S2), and reached maximum transgene expression levels only when continuously induced for over 2.5 hr (Figure 2E). While the pH-Sensor was able to reliably detect the current culture pH with high precision, it could also be used to induce desired transgene expression by addition of different types of acids, including 3-hydroxybutyric acid, one of the key organic acids responsible for DKA (Figure 2F). Comparative analysis of transiently transfected, stable polyclonal, and stable monoclonal pH-Sensor cell lines showed similar half-maximum activation and induction kinetics (Figure S3).

To quantitatively analyze robustness and functional predictability of the pH-Sensor device and its subsequent variants, we developed a dynamic, multiscale mathematical model for engineered HEK293 cells and their—in vitro or in vivo—environment (see Supplemental Information and Figures S4 and S5 for all

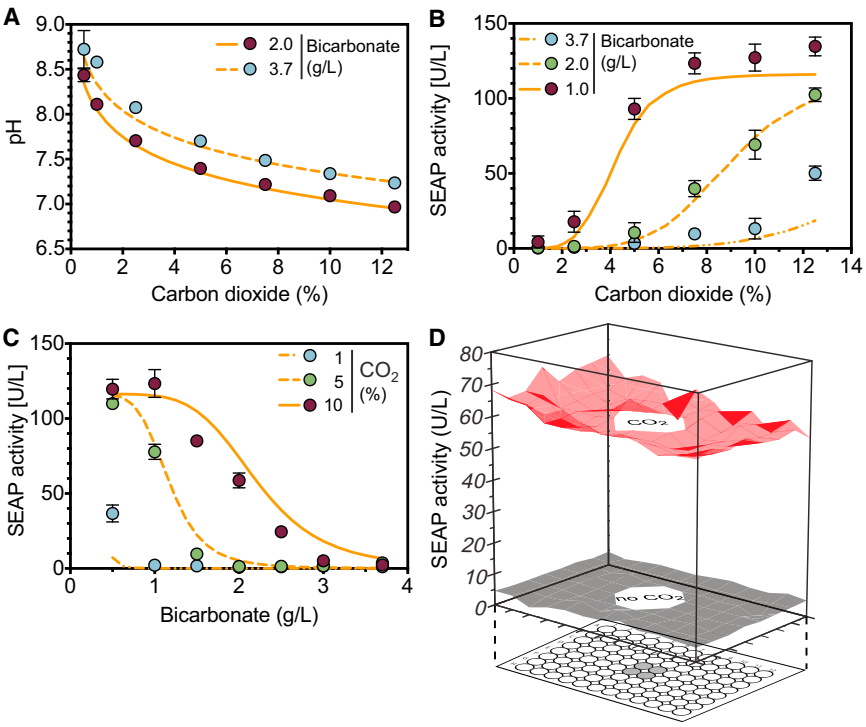

Figure 3. CO_2ntrol-Mediated Transgene Induction Characteristics

(A) pH of cell culture medium exposed to different CO_2 atmospheres. Standard cell culture medium containing 2 g/l and 3.7 g/l bicarbonate was maintained in normal cell culture incubators set to different percent CO_2 content of the atmosphere inside, and the resulting culture pH was assessed using SensorDish technology.

(B and C) Experimental validation of CO_2ntrol performance. pH-Sensor-engineered HEK293 cells were exposed to varying CO_2 (B) and bicarbonate (C) concentrations, and SEAP production was profiled in the culture supernatant after 24 hr.

(D) Dry ice-based gaseous CO_2-triggered induction of the pH-Sensor device. 5×10^4 pH-Sensor-engineered HEK293 cells seeded per well of a 96-well plate were exposed to CO_2-sublimating dry ice (1 g) placed in the four central wells, and SEAP levels were assessed in the culture supernatants after 24 hr (red). A noninduced, dry-ice-free setting was used as control (black). Orange curves indicate corresponding model-based simulations. Data presented are mean ± SEM, n ≥ 3. See also Figures S4 and S5.

details). Briefly, the synthetic circuit model represents TDAG8-mediated pH sensing, intracellular signaling, gene expression control, and cell physiology. The model is able to well capture the system behavior under different experimental conditions (Figures 2B–2E) using a single consistent parametrization. It also reconciles the apparent contradiction between SEAP dynamics in Figure 2D (continuous increase) and Figure 2E (plateau for long pulses) by considering adaptation of the natural signaling pathway. Overall, the pH-Sensor provides the technology for trigger-inducible product gene expression and shows all critical, quantitative performance characteristics that are required to serve as a physiologic acidosis sensor device.

CO_2ntrol

In the CO_2-bicarbonate buffering system in aqueous solutions, cell culture pH, bicarbonate, and CO_2 directly correlate. Therefore, standard cell culture as well as industrial bioprocesses tailored to biopharmaceutical manufacturing of protein therapeutics control pH in culture dishes as well as in bioreactors by gaseous CO_2. When exposing cell culture medium containing fixed bicarbonate levels to different concentrations of gaseous CO_2, the resulting pH could be profiled in culture medium in real time using a SensorDish Reader, confirming that pH of cell culture medium could be precisely adjusted by gaseous CO_2 (Figure 3A). In particular, carbon dioxide-inducible transgene control (CO_2ntrol)-mediated transgene transcription positively correlated with increasing CO_2 levels, while the bicarbonate concentration set the amount of CO_2 required for maximum expression levels. CO_2ntrol-mediated SEAP expression of pH-Sensor-transfected HEK293 ($HEK_{pH\text{-}Sensor}$, pDA62/pCK53) confirmed bicarbonate-determined CO_2-triggered maximum SEAP production levels, and the mathematical model captured this behavior consistently (Figures 3B and 3C). While one can adjust the CO_2 levels of the incubator to fine-tune desired transgene expression, gas-inducible transcription control could also be confirmed by placing dry-ice pellets into the four central wells of a 96-well plate containing $HEK_{pH\text{-}Sensor}$ in all remaining wells (Figure 3D). CO_2 rapidly sublimates from the dry-ice pellets and redissolves into neighboring wells, thereby acidifying the culture medium and boosting SEAP production (Figure 3D). Thus, CO_2ntrol enabled precise programmable, adjustable, and traceless gas-inducible transgene expression in mammalian cells.

Atmosphere-Programmable Logic Gates

We confirmed the compatibility of the pH-Sensor with state-of-the-art small molecule-responsive transcription control devices by engineering a series of gas-programmable two-input logic gates (Figure 4). When the erythromycin-repressible transcription regulation and CO_2ntrol systems are set to drive GFP expression, the reporter output exhibits *A implies B* expression logic when exposing engineered HEK293 to different combinations of inducing erythromycin concentrations (input *A*, 2.7 μM) and CO_2 levels in the culture atmosphere (input *B*, 20%) (Figure 4A; Figure S6D). According to a validated split transcription factor heterodimerization design, CO_2-controlled expression of VP16-DocS complemented with constitutively expressed TtgR-Coh2 resulted in a synthetic transcription factor capable of activating P_{TtgR1} promoters (Nissim and Bar-Ziv, 2010). In response to different combinations of inducing phloretin concentrations (input *A*, 50 μM) and CO_2 levels in the culture atmosphere (input *B*, 20%), this network topology shows typical *B ANDNOT A* input signal processing (Figure 4B; Figure S6E).

Dual gas-programmable logic gates were designed by combining CO_2ntrol with the acetaldehyde-inducible regulation (AIR) system (Weber et al., 2004). Correspondingly engineered cells produce an *OR*-type expression logic characterized by reporter production when either or both gases in the culture atmosphere reach inducing levels (acetaldehyde, 60 ppm; CO_2, 20%) (Figure 4C; Figure S6F). When daisy-chaining both gas-control devices in a way that CO_2ntrol drives expression of AlcR, which induces GFP expression, specific dual-gas input results in *AND* expression logic, which produces a fluorescence output only when the engineered HEK293 cells sense both signals (acetaldehyde, 60 ppm; CO_2, 20%) (Figure 4D; Figure S6G). Cells producing constitutive GFP were inert to any input variation (Figure S6A).

CO_2-Remote-Controlled Gene Expression in Human Cells Grown Inside Microfluidic Devices

Most microfluidic cell culture devices are made of polymerized polydimethylsiloxane (PDMS) (Young and Beebe, 2010). To evaluate whether CO_2 can permeate the PDMS matrix to remote-control transgene expression of engineered cells inside a sealed microfluidic device, we developed a microfluidic chip that contains three parallel cell culture chambers for simultaneous real-time microscopic analysis of up to three different cell populations under identical culture conditions (Figures 5A and 5B). Microfluidic chips containing HEK293 cells engineered for CO_2ntrol-mediated TurboGFP-dest1 (tGFP) expression in two chambers and the same number of control cells constitutively expressing the reporter construct in the third cell culture chamber were used to expose the cells for 48 hr to atmospheres adjusted to high (14%) and low (5%) CO_2 concentrations, and reporter expression was recorded by time-lapse fluorescence microscopy. While tGFP expression remained shut down at 5% CO_2 (Figure 5C; Movie S1) and was induced and visible 4 hr after induction in a 14% CO_2 atmosphere (Figure 5D; Movie S1), constitutive reporter gene expression remained identical at high and low CO_2 (Movie S2). Dynamic studies in which reporter gene expression was first repressed for 24 hr at 5% CO_2 and then induced for 24 hr at 14% CO_2 (Figure 5E; Movie S3), or first induced by a 6 hr 14% CO_2 exposure reaching peak expression at 12 hr followed by a 42 hr shut down period at 5% CO_2, during which tGFP was degraded via its PEST domain (Figure 5F; Movie S3), confirmed that cellular behavior could be remote-controlled through the gas-permeable PDMS of the microfluidic device.

CO_2ntrol-Based Production of Rituximab in Protein-Free Suspension Cultures Grown in Stirred-Tank Bioreactors

State-of-the-art industrial bioreactors control proton levels of the production culture using base and gaseous CO_2 influx (Figure 6A). In a prototype biopharmaceutical manufacturing scenario, we cultivated pH-Sensor-transgenic FreeStyle 293F suspension cells in protein-free, chemically defined culture medium using a reference stirred-tank bioreactor to remote-control and program product gene expression to desired levels using gaseous CO_2. We increased or decreased CO_2 influx or base pump activity at specific time points, which resulted in predefined pH changes of the production medium and adjusted expression of SEAP (Figure 6B) or of the blockbuster biopharmaceutical Rituximab (Figure 6C). The CO_2-triggered pH changes in the production medium correlated with changes in specific SEAP/Rituximab productivity. This confirms the functionality of our devices in a proof-of-concept biopharmaceutical manufacturing setting using an industry-approved, FDA-licensed, and traceless trigger compound to time and remote-control product gene expression in bioreactors without creating any downstream processing, validation, or approval challenges.

pH-Guard, a Prosthetic Network Correcting Diabetic Ketoacidosis and Restoring Glucose Homeostasis in Type 1 Diabetes

The CO_2-bicarbonate buffering system keeps normal blood and tissue pH within a very narrow range (pH 7.35–7.45). A tissue pH below 7.35 is known as acidosis, a medical condition that is difficult to diagnose due to its wide range of symptoms and diverse pathophysiologies. To validate in vivo performance and precision of the pH-Sensor, which was able to discern normal (>7.35) and pathologic (<7.35) pH in mammalian cell cultures (Figure 2B), we implanted alginate-microencapsulated $HEK_{pH\text{-}Sensor}$ into wild-type and acidotic mice. Providing insulation, immunoprotection, and vascularization, alginate has become a preferred encapsulation material for in vivo implantation of mammalian cells and was recently validated in a human clinical trial showing sustained function of intraperitoneally implanted alginate-encapsulated human islet cells in type 1 diabetic patients (Jacobs-Tulleneers-Thevissen et al., 2013). Treatment of animals for 5 days with the carbonic anhydrase inhibitor acetazolamide (ACA), a clinically licensed drug (Diamox) for the treatment of glaucoma, epileptic seizures, and intercranial hypertension, has been shown to induce metabolic acidosis (Raghunand et al., 2003). Because blood SEAP levels were significantly increased in acidotic mice compared to wild-type animals (Figure S7A), pH-Sensor implants were able to tap into the animals' circulation, monitor proton levels, process pH information, and trigger a transgene expression response resulting in SEAP secretion and accumulation in the bloodstream. In vitro control experiments confirmed that the capsule structure was inert to low pH and facilitated diffusion of SEAP produced by encapsulated cells in response to low pH (Figures S7B and S7C).

With the pH-Sensor functionality validated in mice, we designed a prosthetic network for the treatment of DKA. By functionally linking the sensor module (pDA62) to expression of secretion-engineered furin-cleavable proinsulin 1 (effector module: pDA145; P_{CRE}-mIns-pA), enabling efficient insulin maturation and secretion in non-β cells (Hay and Docherty, 2003), we created the prosthetic network pH-Guard. Transgenic cells ($HEK_{pH\text{-}Guard}$) were expected to sense DKA via low pH and produce an insulin secretion response that reduces ketosis and restores physiologic pH and glucose homeostasis.

Type 1 diabetic mice showed undetectable insulin levels (Figure S7D), high 3-hydroxybutyrate levels (Figure S7E), hyperglycemia (Figure S7F), and low bicarbonate concentrations (Figure S7G) in the blood as well as high glucose (>55 mmol/l) and acetoacetic acid (>15 mmol/l) concentrations in the urine.

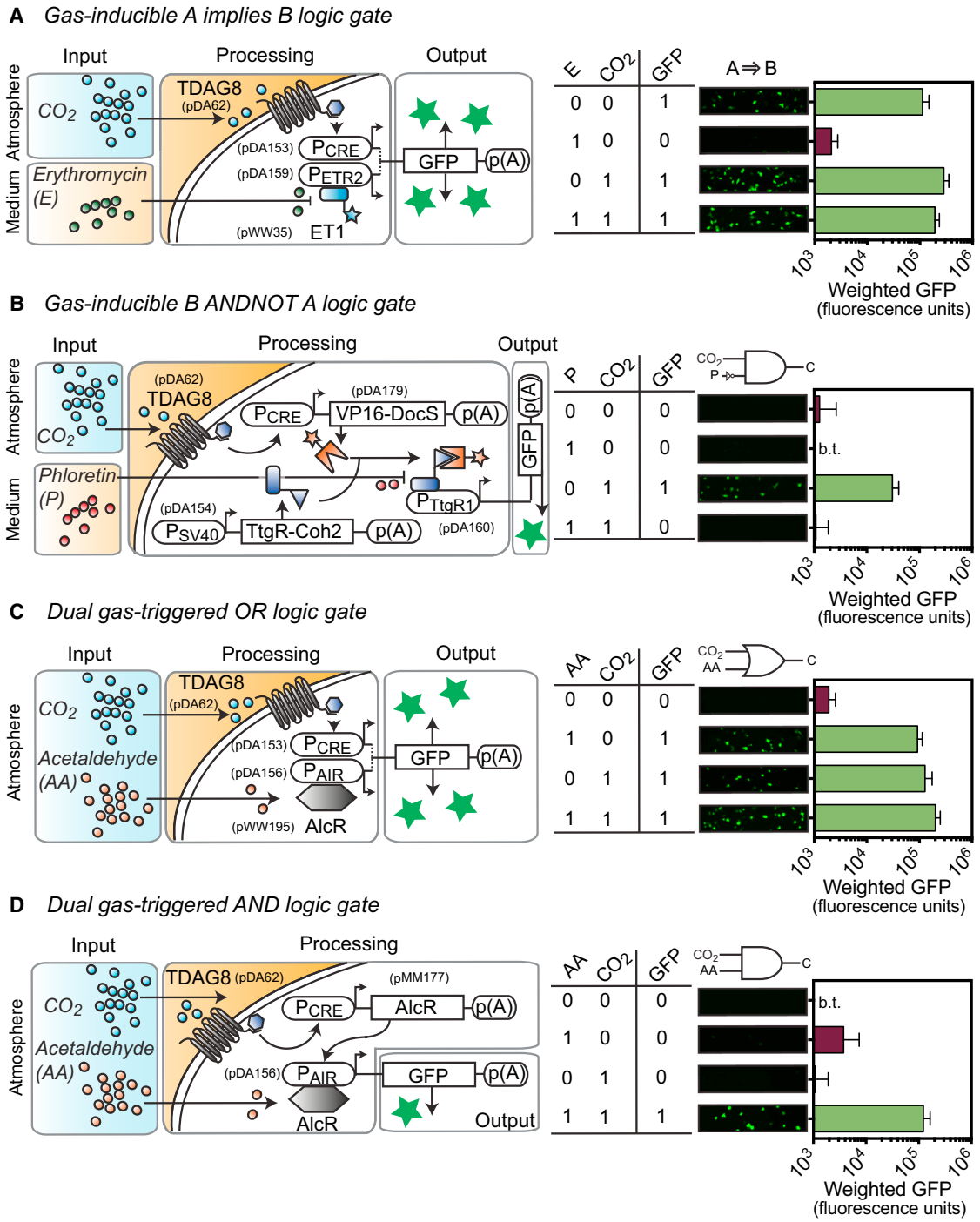

Figure 4. CO_2ntrol-Programmable Logic Gates

(A) Gas-controlled *A implies B* logic gate. When combining the CO_2ntrol device and the erythromycin-repressible transcription control system, as shown in the genetic switchboard, and supplying inducing concentrations of CO_2 (20%) and erythromycin (2.7 μM) according to the truth table, engineered cells produce GFP except for the exclusive presence of erythromycin, as shown by fluorescence microscopy and FACS analysis.

(B) Gas-controlled *B ANDNOT A* logic gate. Following split expression according to the genetic switchboard, the synthetic split transcription factor TtgR-Coh2-DocS-VP16 induces P_{TtgR1}-driven GFP expression in a phloretin-repressible manner. Combining inducing concentrations of the two input signals, CO_2 (20%) and phloretin (50 μM), according to the truth table programs transfected HEK293 cells to produce the fluorescent output exclusively at inducing levels of atmospheric CO_2.

(legend continued on next page)

When implanting $HEK_{pH\text{-}Sensor}$, the animals had increased SEAP serum levels, confirming that they were indeed suffering from DKA (Figure S7H). Also, prevalidation of pH-Guard in cell culture confirmed that cells secrete high doses of insulin at acidosis-relevant pH (Figure 7A; EC_{50} = pH 7.18 ± 0.04). Upon implantation of microencapsulated batches of the same $HEK_{pH\text{-}Guard}$ cell population into mice suffering from DKA, these mice produced an efficient systemic insulin response, with insulin levels matching those of healthy control mice that have their insulin production tuned by the native pancreatic β cell population (Figure 7B). As a consequence of systemic insulin production, ketosis was reduced and 3-hydroxybutyrate levels decreased significantly (Figure S7I). Also, while untreated mice suffering from type 1 diabetes showed dramatic hyperglycemia, blood glucose levels in animals with pH-Guard implants were similar to healthy control mice (Figure 7C). With pH-Guard, type 1 diabetic mice also showed reduced glycemic excursions in glucose tolerance tests, albeit with a slower response than healthy mice (Figure 7D). To evaluate the full physiological response, we employed our dynamic mathematical model for predictions of tolerance test dynamics (Figure 7E) and of responses to implantation of pH-Guard (Figure 7F) in mice ranging from type 1 diabetic to normal. In both scenarios, pH-Guard is predicted to robustly restore normal physiology with respect to blood pH, bicarbonate, insulin, and glucose, irrespective of the degree of simulated diabetes (or absence thereof). More specifically, our network will counteract physiological excursions on the timescales required to prevent severe DKA (1) by providing basal insulin production to counter short-term increases in glucose concentrations (Figures 7D and 7E) and (2) by highly sensitive responses under conditions of severe acidosis, with fast (<6 hr) initial adaptation to mild acidosis conditions and slower reconstitution of normal physiology (Figure 7F). Hence, experiments and model predictions confirm that pH is an appropriate surrogate physiology signal; closed-loop operation of pH-Guard's insulin-based effector device restores glucose homeostasis in treated animals, and the device has the clinically relevant characteristics to prevent severe diabetic acidosis.

DISCUSSION

Trigger-inducible transcription control of heterologous transgenes has become standard practice in gene-function analysis (Wiznerowicz et al., 2006), functional genomic research (Baumgärtel et al., 2008), drug discovery (Weber et al., 2008), and biopharmaceutical manufacturing of difficult-to-produce protein therapeutics (Weber and Fussenegger, 2007), as well as prototype gene and cell-based therapies (Wieland and Fussenegger, 2012). During the past years, gene switch-based designer circuits have also successfully been tested in animal models of human disorders, which fosters advances of future treatment strategies. Pioneering examples include remote-controlled transgene expression in engineered cell implants using electromagnetic waves in the visible or radio-frequency range (Stanley et al., 2012; Ye et al., 2011) or transdermal control by beauty creams (Gitzinger et al., 2009). The most recent generation of therapeutic designer circuits such as the ones tailored for the treatment of gouty arthritis (Kemmer et al., 2010) and obesity (Rössger et al., 2013b) function as a prosthetic network that monitors metabolic disturbances, processes such signals, and coordinates a therapeutic response in an automatic and self-sufficient manner.

The pH-Sensor device reported here provides a precise approach to transgene-transcription control in mammalian cells. The pH-Sensor can either be induced by increasing the amount of protons in solution by addition of (in)organic acids or by shifting the ubiquitous CO_2-bicarbonate buffering system to lower pH (higher hydrogen ion levels) using gaseous CO_2. This establishes it as an adjustable and side effect-free gas-inducible transcription control (CO_2ntrol) system that is able to fine-tune product gene expression for biological studies as well as production processes, provides remote-control of cellular behavior inside microfluidic devices, and can be combined with orthogonal transcription-control devices to design gene networks with programmable dual-input expression logic.

The CO_2ntrol technology is particularly suited for biopharmaceutical manufacturing of protein therapeutics. Currently available inducer molecules, such as antibiotics, hormones, and other small-molecule drugs to adjust expression of biopharmaceuticals, are incompatible with licensed downstream-processing procedures and process economics (Weber and Fussenegger, 2007). In contrast, CO_2-based pH control is standard practice in any FDA-licensed biopharmaceutical manufacturing process, promoting the use of CO_2ntrol technology for fine-tuning the production of protein therapeutics.

The pH-Sensor shows high sensitivity and precision, as it is functional within the entire physiologic pH range and significantly induced at pH below 7.35, which marks the transition between normal and pathologic blood pH at the onset of DKA (Kitabchi et al., 2009). Pathologic blood pH is neither reached by moderate alcohol consumption (devoid of alcoholic ketoacidosis) (Langhan, 2013) nor by intense physical exercise (devoid of lactic acidosis) (Kłapcińska et al., 2013; Wasserman et al., 2014). Thus, assuming a normal lifestyle, the pH-Sensor should be activated only during DKA. Conceptually, this implies that pH can be a suitable surrogate signal of the physiological state, provided that it is sensed precisely and selectively. Our closed-loop prosthetic network (pH-Guard) that links

(C) Dual gas-controlled *OR* logic gate. When combining the CO_2ntrol device with the acetaldehyde-inducible gene switch as shown in the genetic switchboard and supplying CO_2 and gaseous acetaldehyde according to the truth table, transfected HEK293 cells produce GFP whenever inducing CO_2 (20%) *or* acetaldehyde concentrations (60 ppm) or both gases are present in the culture atmosphere.
(D) Dual gas-controlled *AND* logic gate. When interconnecting the CO_2ntrol device and the acetaldehyde-inducible gene switch as shown in the genetic switchboard and supplying CO_2 and gaseous acetaldehyde according to the truth table, transfected HEK293 cells produce GFP whenever inducing concentrations of both CO_2 (20%) and acetaldehyde (60 ppm) are present in the culture atmosphere. b.t., below threshold of 10^3 fluorescence units. Representative micrographs are shown. FACS data presented are mean ± SD, n ≥ 3. See also Figure S6.

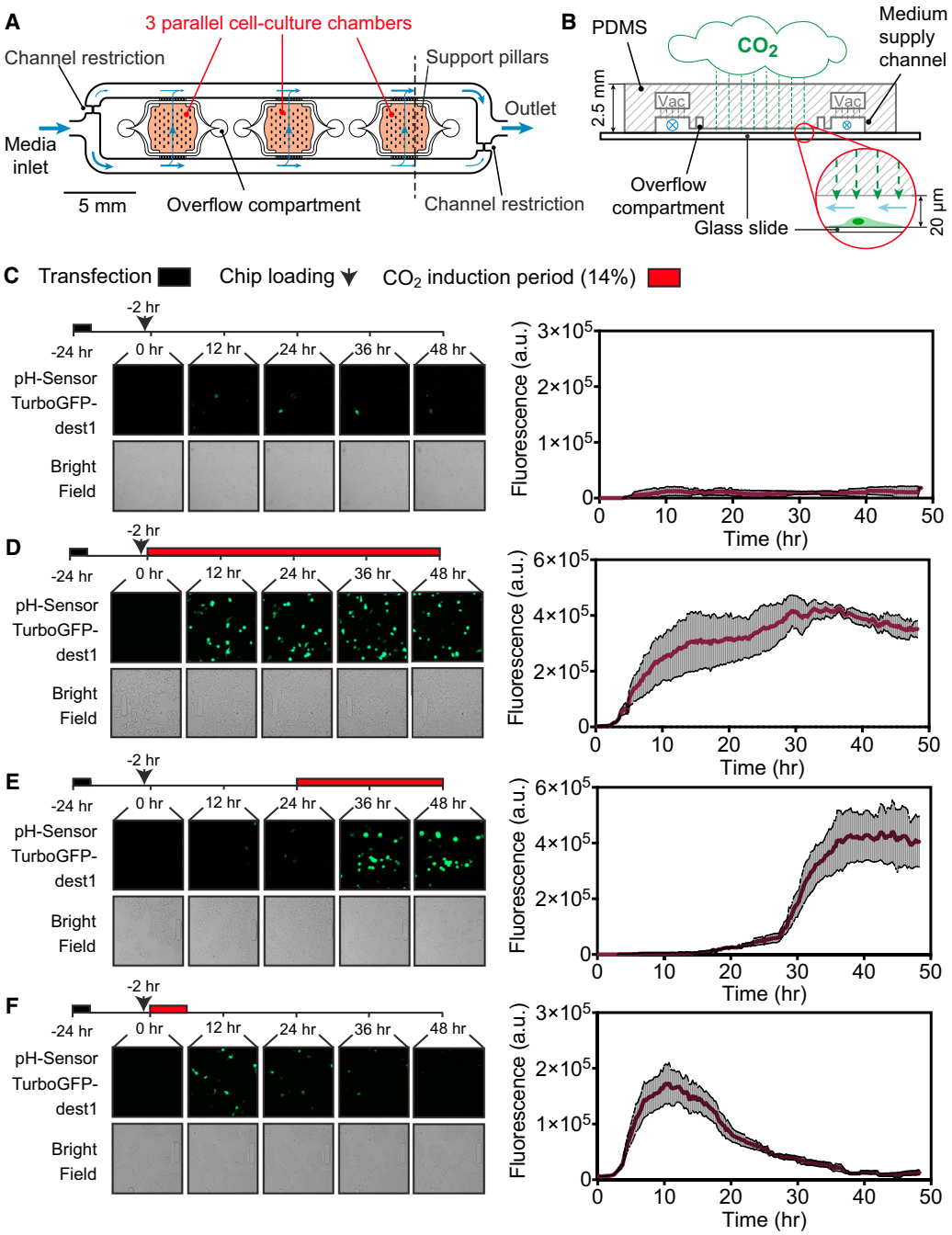

Figure 5. Live-Cell Imaging of CO_2ntrol-Engineered Cells inside Microfluidic Chips

(A) Schematic top view of the microfluidic chip. Three cell culture chambers enable crosstalk-free cultivation of up to three cell populations under identical conditions.

(B) Cross-section of the microfluidic chip (dashed line across schematic top view shown in A). Cells adhere to the glass slide of the 20 µm-high cell culture chamber. The close-up view illustrates the orthogonality of medium and gas exchange in the cell culture chamber. (Heights are not to scale.)

(C–F) Micrographs (left) and time-lapse microscopy-based quantification of cellular fluorescence (right) of CO_2ntrol-engineered HEK293 cells cultivated inside the cell culture chamber of the microfluidic device after incubation in an atmosphere containing (C) low (5%, repressing state) or (D) high (14%, inducing state) CO_2 levels for 48 hr (see also Movie S1). (E) Delayed onset of CO_2-controlled transgene expression. Cell-containing microchips were first incubated for 24 hr in an atmosphere containing 5% and then exposed for another 24 hr to 14% CO_2 to induce fluorescent reporter gene expression (see also Movie S3). (F) Dynamic CO_2-controlled transgene expression switches. Six hours of transient exposure of the microfluidic device to 14% CO_2 programs CO_2ntrol-engineered cells to produce a transient fluorescence response (see also Movie S3). Quantification of fluorescence shows the mean ± SEM of three different positions per run. See also Movies S1, S2, and S3.

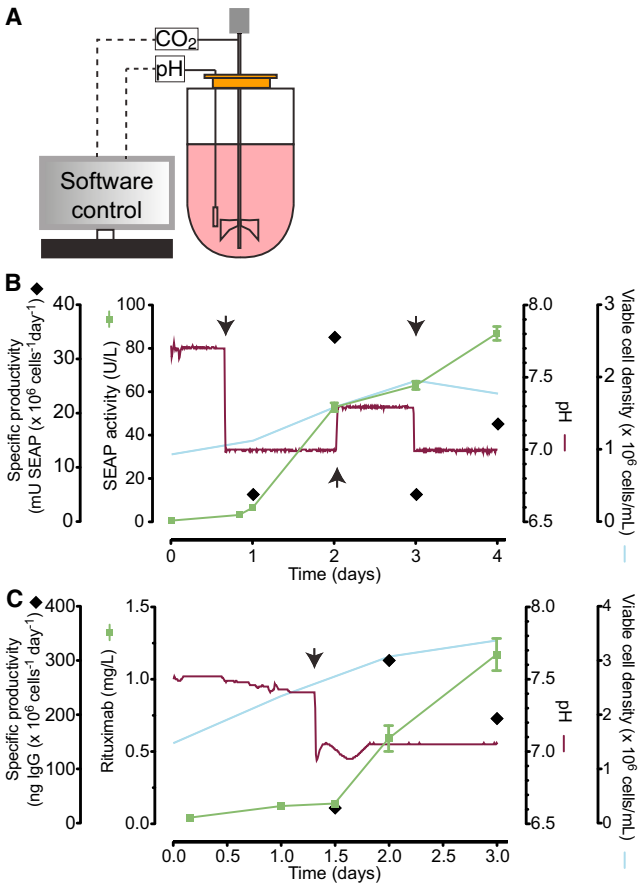

Figure 6. Performance of CO_2ntrol-Mediated Product Gene Expression in Stirred-Tank Bioreactors

(A) Schematic of the stirred-tank bioreactor used for CO_2ntrol-driven product gene expression.

(B) CO_2-programmable SEAP expression in a standard stirred-tank bioreactor. pH-Sensor-transgenic (pDA55/pCK53) FreeStyle 293F suspension cells were cultivated in 1 l protein-free, chemically defined medium using a stirred-tank bioreactor, and SEAP production was programmed by shifts in gaseous CO_2 influx (arrows).

(C) CO_2ntrol-programmed production of the blockbuster anticancer drug Rituximab. FreeStyle 293F suspension cells transgenic for pH-Sensor-driven Rituximab production (pDA55/pDA146) were cultivated in 1.4 l protein-free, chemically defined medium using a stirred-tank bioreactor, and Rituximab production was induced by a shift in gaseous CO_2 influx (arrow). Data presented are mean ± SEM of a representative bioreactor run. Product protein concentration was quantified in triplicate.

pH-Sensor to expression of a secretion-engineered insulin variant provides a corresponding proof-of-concept that the network senses DKA in mice, corrects the acidotic state, and restores glucose homeostasis. DKA remains an important cause of death in people with T1DM (Henriksen et al., 2007). The pathophysiological mechanism for the development of DKA is an absolute or relative lack of insulin due to forgotten insulin injections or deficient insulin treatment in situations with considerably increased insulin requirements such as infections and sepsis (Van Cromphaut et al., 2008). In patients at high risk for recurring DKA (Randall et al., 2011), such a prosthetic network could become a life-saving protective measure. Besides designing medical devices that combine glucose sensing with insulin-delivery pumps (Hovorka, 2011), there is consensus to engineer β cell mimetics that provide glucose-sensitive expression of insulin (Bouwens et al., 2013). However, the design of synthetic glucose sensor circuitry matching the sensitivity of blood glucose levels remains a challenge. The indirect glucose sensing and coordinated insulin production of pH-Guard may represent a first example for such a closed-loop prosthetic glucose homeostasis network. The diagnostic criteria for DKA suggested by the American Diabetes Association consensus statement (Kitabchi et al., 2009) differentiates three levels of severity (mild, moderate, and severe) where mild DKA is characterized by arterial pH between 7.30 and 7.25, exactly the range in which the pH-Sensor becomes active (Figure 2B) and far away from severe DKA, reached at arterial pH of 7.0. Hence, our prosthetic network can detect early stages of DKA and counterbalance against acidosis by secretion of insulin (Figure 7). pH-Guard functionality does not exist in humans, yet the network is entirely built of human components. Due to its modular design, it will be straightforward to replace the sensor/effector componentry and to adapt this prosthetic network strategy to other metabolic disorders and provide treatment concepts for future gene- and cell-based therapies.

EXPERIMENTAL PROCEDURES

Vector Design

Comprehensive design and construction details for all expression vectors are provided in Table S1. Key plasmids include pCK53, which contains a P_{CRE}-driven SEAP expression unit that is induced by CREB1 (P_{CRE}-SEAP-pA). pDA55 and pDA62 encode constitutive expression of TDAG8 driven by the human elongation factor 1 alpha ($P_{hEF1\alpha}$-TDAG8-pA) and simian virus 40 (P_{SV40}-TDAG8-pA) promoters, respectively. pDA145 mediates P_{CRE}-driven expression of a rodent proinsulin 1 harboring a furin cleavage site between B chain and C peptide. pDA146 is a P_{CRE}-driven Rituximab (Rituxan, MabThera) expression vector (P_{CRE}-LC_R-$IRES_{EMCV}$-HC_R-pA; LC_R/HC_R Rituximab heavy and light chains, $IRES_{EMCV}$, internal ribosome entry site derived from the encephalomyocarditis virus). pDA153 is a P_{CRE}-driven GFP expression plasmid (P_{CRE}-TurboGFP-dest1-pA).

Mammalian Cell Culture and Transfection

Human embryonic kidney cells (HEK293T, ATCC: CRL-11268) and human bone marrow stromal cells transgenic for the catalytic subunit of human telomerase (hMSC-TERT) (Simonsen et al., 2002) were cultured in Dulbecco's modified Eagle's medium (DMEM, Invitrogen) supplemented with 10% fetal calf serum (FCS, Bioconcept, lot no. PE01026P) and 1% penicillin/streptomycin solution (Sigma-Aldrich). Chinese hamster ovary cells (CHO-K1, ATCC: CCL-61) were grown in ChoMaster HTS (Cell Culture Technologies) supplemented with 5% FCS and 1% penicillin/streptomycin solution. FreeStyle 293-F suspension cells (Life Technologies Corporation, cat. no. R790-07) were cultivated in FreeStyle 293 Expression Medium (Life Technologies Corporation, cat. no. 12338018) supplemented with 1% penicillin/streptomycin solution and grown in shake flasks placed on an orbital shaker set to 100–150 rpm (IKA KS 260 basic, IKA-Werke GmbH). Unless stated otherwise, all cell types were cultivated at 37°C in a humidified atmosphere containing 5% CO_2. Cell number and viability were quantified using an electric field multichannel cell counting device (Casy Cell Counter and Analyzer Model TT, Roche Diagnostics GmbH). For transfection, a solution containing 0.5 μg plasmid DNA (1 μg for FreeStyle 293-F) and 3 μl PEI (1 mg/ml) was incubated in 0.2 ml FCS-free DMEM for 30 min at 22°C before it was added dropwise to 1 × 10^5 cells (1 × 10^6 FreeStyle 293-F) seeded per well of a 24-well plate

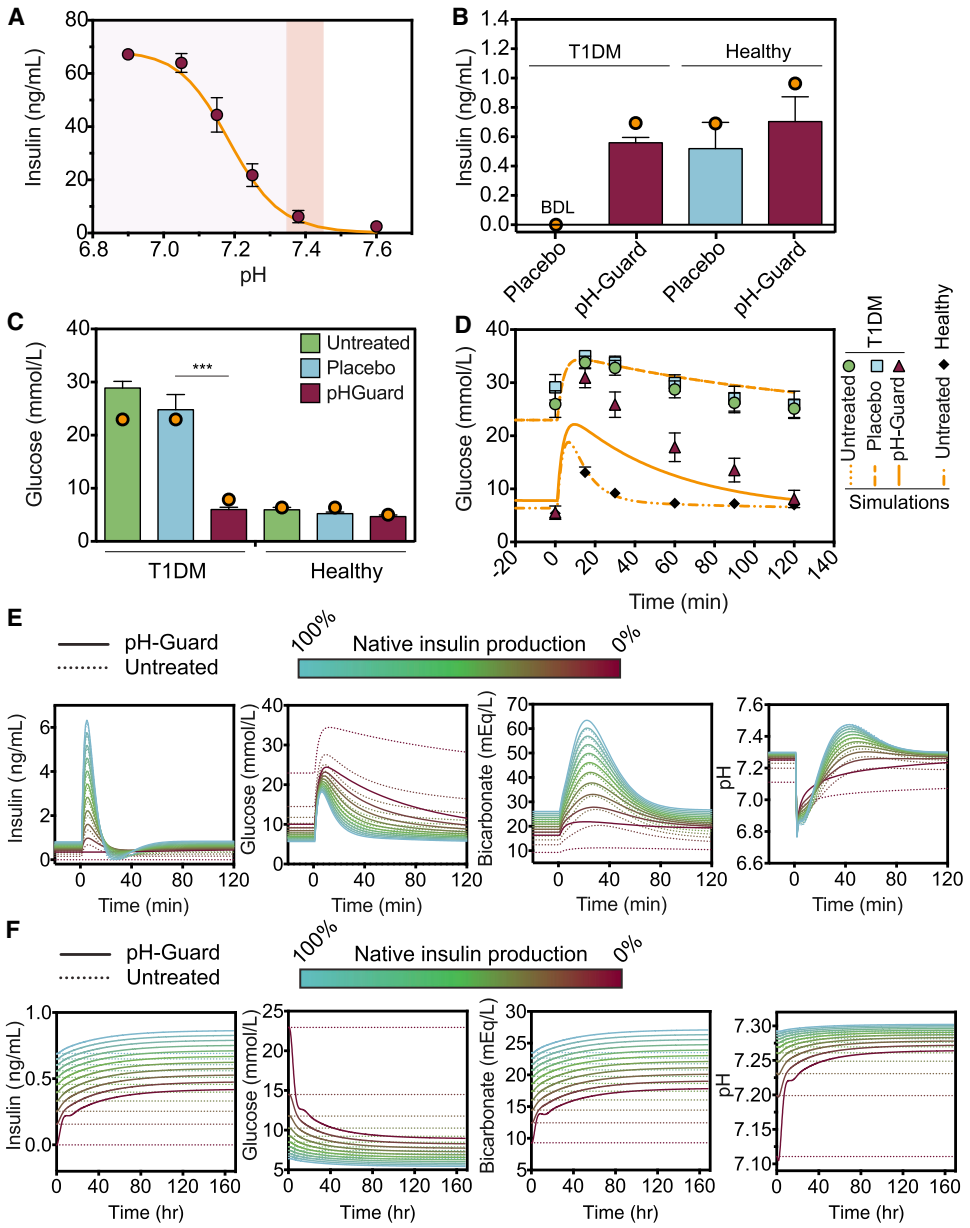

Figure 7. Design, Characterization and In Vivo Validation of pH-Guard, a Safeguard Device for the Treatment of Diabetic Ketoacidosis and Type 1 Diabetes Mellitus (T1DM)

(A) pH-Guard performance in cell culture. pH-Guard-transgenic pDA62-/pDA145-engineered HEK293 cells ($HEK_{pH\text{-}Guard}$) were grown for 24 hr in cell culture medium adjusted to different pH before insulin production was profiled in the culture supernatant. Red translucent background represents the narrow range of human blood pH (pH 7.35–7.45) while the gray transparent background indicates pH values associated with human acidosis (pH < 7.35). EC_{50} = 7.18 ± 0.04.

(B) pH-Guard performance in mice. Mice suffering from type 1 diabetes mellitus (T1DM) were implanted with $HEK_{pH\text{-}Guard}$, and blood insulin levels were profiled after 24 hr. T1DM mice receiving placebo implants and healthy animals treated with placebo and pH-Guard implants served as controls. Insulin levels in placebo-implanted T1DM mice were below detection limit (BDL; < 0.1 ng/ml).

(C) pH-Guard-based control of glucose homeostasis in T1DM mice. Blood glucose levels were quantified in T1DM mice 24 hr after treatment with pH-Guard implants. Untreated and placebo-implanted T1DM mice as well as healthy animals receiving placebo and pH-Guard implants served as controls.

(D) Impact of pH-Guard implants on glucose tolerance. T1DM mice treated with pH-Guard, placebo, or no implants received intraperitoneal glucose injections, and their subsequent glycemic excursions were recorded. Glucose tolerance of wild-type mice served as control.

(E and F) Model-based predictions of pH-Guard-mediated control of insulin expression dynamics and their effects on blood bicarbonate, glucose, and pH in mice for short-term responses to glucose injection at time zero (E) and for long-term homeostasis (F). Solid lines show pH-Guard-implanted mice and dotted lines indicate untreated animals. The color gradient indicates simulated percent native insulin level ranging from 0% (T1DM) to 100% (wild-type). Orange curves and circles indicate corresponding model-based simulations. See Figure S7 for in-depth characterization of T1DM mice. Data are presented are mean ± SEM; n = 10 mice; statistics by two-tailed t test; ***p < 0.0001. See also Figures S4, S5 and S7.

24 hr before transfection. Unless stated otherwise, the transfection medium was replaced by standard cultivation medium adjusted to specific pH after 7 hr, and transgene expression was profiled after 24 hr.

Implant Production

Cell implants were produced by encapsulating pDA62/pCK53- or pDA62/pDA145-transgenic HEK293 into coherent alginate-(poly-*L*-lysine)-alginate capsules (400 μm, 200 cells/capsule) using an Inotech Encapsulator Research IE-50R (EncapBioSystems) set to the following parameters: 0.2 mm single nozzle, stirrer speed control 5 units, 20 ml syringe with a flow rate of 410 units, nozzle vibration frequency of 1,024 Hz, 900 V for capsule dispersion. Integrity and quality of capsules maintained at different pH were confirmed by microscopy (Figure S7B).

Animal Experiments

For simulation of a metabolic acidosis in wild-type mice, female Swiss Mice (Oncins France souche 1, Charles River) received twice daily intraperitoneal injections of acetazolamide (Sigma, cat. no. A6011; 200 mg/kg in 300 μl PBS) over 5 days. To establish the type 1 diabetes animal model, the mice were fasted for 36 hr and injected with a single dose of alloxan monohydrate (Sigma, cat. no. A7413, 200 mg/kg in 300 μl PBS), while the control treatment group received PBS injections (Federiuk et al., 2004; Wang et al., 2010). Mice that developed type 1 diabetes and DKA after 48 hr showed high glucose levels in the blood (>20 mmol/l) and urine (>55 mmol/l) as well as elevated concentrations of ketone bodies in the blood (3-hydroxybutyrate > 2 mmol/l) and the urine (acetoacetic acid > 15 mmol/l). Mice were intraperitoneally implanted with 2–5 × 10^6 microencapsulated transgenic cells (1 × 10^4 capsules in 0.7 ml serum-free DMEM). After 24 hr, blood samples were collected and the serum was isolated using microtainer SST tubes (Becton Dickinson) according to the manufacturer's protocol. All experiments involving mice were performed according to the directives of the European Community Council (2010/63/EU), approved by the French Republic (N°69266309), and carried out by G.C.-E.H. at the Institut Universitaire de Technology, IUTA, 69622 Villeurbanne Cedex, France.

SUPPLEMENTAL INFORMATION

Supplemental Information includes Supplemental Discussion, Supplemental Experimental Procedures, seven figures, three tables, and three movies and can be found with this article online at http://dx.doi.org/10.1016/j.molcel.2014.06.007.

ACKNOWLEDGMENTS

We thank A. Schulz, P. Saxena, T. Horn, and H. Zulewski for providing plasmids and generous advice. This work was supported by an ERC advanced grant (no. 321381) and in part by the INTERREG IV A.20 and the Gutenberg Chair awarded to M.F.

Received: December 20, 2012
Revised: March 7, 2014
Accepted: May 15, 2014
Published: July 10, 2014

REFERENCES

Ausländer, S., Ausländer, D., Müller, M., Wieland, M., and Fussenegger, M. (2012). Programmable single-cell mammalian biocomputers. Nature *487*, 123–127.

Bacchus, W., Lang, M., El-Baba, M.D., Weber, W., Stelling, J., and Fussenegger, M. (2012). Synthetic two-way communication between mammalian cells. Nat. Biotechnol. *30*, 991–996.

Barker, J.M., Goehrig, S.H., Barriga, K., Hoffman, M., Slover, R., Eisenbarth, G.S., Norris, J.M., Klingensmith, G.J., and Rewers, M.; DAISY study (2004). Clinical characteristics of children diagnosed with type 1 diabetes through intensive screening and follow-up. Diabetes Care *27*, 1399–1404.

Baumgärtel, K., Genoux, D., Welzl, H., Tweedie-Cullen, R.Y., Koshibu, K., Livingstone-Zatchej, M., Mamie, C., and Mansuy, I.M. (2008). Control of the establishment of aversive memory by calcineurin and Zif268. Nat. Neurosci. *11*, 572–578.

Bouwens, L., Houbracken, I., and Mfopou, J.K. (2013). The use of stem cells for pancreatic regeneration in diabetes mellitus. Nat. Rev. Endocrinol. *9*, 598–606.

Casey, J.R., Grinstein, S., and Orlowski, J. (2010). Sensors and regulators of intracellular pH. Nat. Rev. Mol. Cell Biol. *11*, 50–61.

Chen, Y.Y., Jensen, M.C., and Smolke, C.D. (2010). Genetic control of mammalian T-cell proliferation with synthetic RNA regulatory systems. Proc. Natl. Acad. Sci. USA *107*, 8531–8536.

Federiuk, I.F., Casey, H.M., Quinn, M.J., Wood, M.D., and Ward, W.K. (2004). Induction of type-1 diabetes mellitus in laboratory rats by use of alloxan: route of administration, pitfalls, and insulin treatment. Comp. Med. *54*, 252–257.

Gitzinger, M., Kemmer, C., El-Baba, M.D., Weber, W., and Fussenegger, M. (2009). Controlling transgene expression in subcutaneous implants using a skin lotion containing the apple metabolite phloretin. Proc. Natl. Acad. Sci. USA *106*, 10638–10643.

Hay, C.W., and Docherty, K. (2003). Enhanced expression of a furin-cleavable proinsulin. J. Mol. Endocrinol. *31*, 597–607.

Henriksen, O.M., Prahl, J.B., Røder, M.E., and Svendsen, O.L. (2007). Treatment of diabetic ketoacidosis in adults in Denmark: a national survey. Diabetes Res. Clin. Pract. *77*, 113–119.

Hovorka, R. (2011). Closed-loop insulin delivery: from bench to clinical practice. Nat. Rev. Endocrinol. *7*, 385–395.

Ishii, S., Kihara, Y., and Shimizu, T. (2005). Identification of T cell death-associated gene 8 (TDAG8) as a novel acid sensing G-protein-coupled receptor. J. Biol. Chem. *280*, 9083–9087.

Jacobs-Tulleneers-Thevissen, D., Chintinne, M., Ling, Z., Gillard, P., Schoonjans, L., Delvaux, G., Strand, B.L., Gorus, F., Keymeulen, B., and Pipeleers, D.; Beta Cell Therapy Consortium EU-FP7 (2013). Sustained function of alginate-encapsulated human islet cell implants in the peritoneal cavity of mice leading to a pilot study in a type 1 diabetic patient. Diabetologia *56*, 1605–1614.

Kemmer, C., Gitzinger, M., Daoud-El Baba, M., Djonov, V., Stelling, J., and Fussenegger, M. (2010). Self-sufficient control of urate homeostasis in mice by a synthetic circuit. Nat. Biotechnol. *28*, 355–360.

Khalil, A.S., and Collins, J.J. (2010). Synthetic biology: applications come of age. Nat. Rev. Genet. *11*, 367–379.

Kitabchi, A.E., Umpierrez, G.E., Murphy, M.B., Barrett, E.J., Kreisberg, R.A., Malone, J.I., and Wall, B.M. (2001). Management of hyperglycemic crises in patients with diabetes. Diabetes Care *24*, 131–153.

Kitabchi, A.E., Umpierrez, G.E., Miles, J.M., and Fisher, J.N. (2009). Hyperglycemic crises in adult patients with diabetes. Diabetes Care *32*, 1335–1343.

Kłapcińska, B., Waśkiewicz, Z., Chrapusta, S.J., Sadowska-Krępa, E., Czuba, M., and Langfort, J. (2013). Metabolic responses to a 48-h ultra-marathon run in middle-aged male amateur runners. Eur. J. Appl. Physiol. *113*, 2781–2793.

Langhan, M.L. (2013). Acute alcohol intoxication in adolescents: frequency of respiratory depression. J. Emerg. Med. *44*, 1063–1069.

Larsen, J.L. (2004). Pancreas transplantation: indications and consequences. Endocr. Rev. *25*, 919–946.

Ludwig, M.G., Vanek, M., Guerini, D., Gasser, J.A., Jones, C.E., Junker, U., Hofstetter, H., Wolf, R.M., and Seuwen, K. (2003). Proton-sensing G-protein-coupled receptors. Nature *425*, 93–98.

Marguet, P., Balagadde, F., Tan, C., and You, L. (2007). Biology by design: reduction and synthesis of cellular components and behaviour. J. R. Soc. Interface *4*, 607–623.

Nissim, L., and Bar-Ziv, R.H. (2010). A tunable dual-promoter integrator for targeting of cancer cells. Mol. Syst. Biol. *6*, 444.

Pickup, J.C. (2012). Management of diabetes mellitus: is the pump mightier than the pen? Nat. Rev. Endocrinol. *8*, 425–433.

Pozzilli, P. (2012). Type 1 diabetes mellitus in 2011: Heterogeneity of T1DM raises questions for therapy. Nat. Rev. Endocrinol. *8*, 78–80.

Raghunand, N., Howison, C., Sherry, A.D., Zhang, S., and Gillies, R.J. (2003). Renal and systemic pH imaging by contrast-enhanced MRI. Magn. Reson. Med. *49*, 249–257.

Randall, L., Begovic, J., Hudson, M., Smiley, D., Peng, L., Pitre, N., Umpierrez, D., and Umpierrez, G. (2011). Recurrent diabetic ketoacidosis in inner-city minority patients: behavioral, socioeconomic, and psychosocial factors. Diabetes Care *34*, 1891–1896.

Rössger, K., Charpin-El Hamri, G., and Fussenegger, M. (2013a). Reward-based hypertension control by a synthetic brain-dopamine interface. Proc. Natl. Acad. Sci. USA *110*, 18150–18155.

Rössger, K., Charpin-El-Hamri, G., and Fussenegger, M. (2013b). A closed-loop synthetic gene circuit for the treatment of diet-induced obesity in mice. Nat Commun *4*, 2825.

Simonsen, J.L., Rosada, C., Serakinci, N., Justesen, J., Stenderup, K., Rattan, S.I., Jensen, T.G., and Kassem, M. (2002). Telomerase expression extends the proliferative life-span and maintains the osteogenic potential of human bone marrow stromal cells. Nat. Biotechnol. *20*, 592–596.

Stanley, S.A., Gagner, J.E., Damanpour, S., Yoshida, M., Dordick, J.S., and Friedman, J.M. (2012). Radio-wave heating of iron oxide nanoparticles can regulate plasma glucose in mice. Science *336*, 604–608.

Tigges, M., Marquez-Lago, T.T., Stelling, J., and Fussenegger, M. (2009). A tunable synthetic mammalian oscillator. Nature *457*, 309–312.

Tominaga, M., Caterina, M.J., Malmberg, A.B., Rosen, T.A., Gilbert, H., Skinner, K., Raumann, B.E., Basbaum, A.I., and Julius, D. (1998). The cloned capsaicin receptor integrates multiple pain-producing stimuli. Neuron *21*, 531–543.

Tresguerres, M., Buck, J., and Levin, L.R. (2010). Physiological carbon dioxide, bicarbonate, and pH sensing. Pflugers Arch. *460*, 953–964.

Van Cromphaut, S.J., Vanhorebeek, I., and Van den Berghe, G. (2008). Glucose metabolism and insulin resistance in sepsis. Curr. Pharm. Des. *14*, 1887–1899.

Waldmann, R., Champigny, G., Bassilana, F., Heurteaux, C., and Lazdunski, M. (1997). A proton-gated cation channel involved in acid-sensing. Nature *386*, 173–177.

Wang, M.Y., Chen, L., Clark, G.O., Lee, Y., Stevens, R.D., Ilkayeva, O.R., Wenner, B.R., Bain, J.R., Charron, M.J., Newgard, C.B., and Unger, R.H. (2010). Leptin therapy in insulin-deficient type I diabetes. Proc. Natl. Acad. Sci. USA *107*, 4813–4819.

Wasserman, K., Cox, T.A., and Sietsema, K.E. (2014). Ventilatory regulation of arterial H(+) (pH) during exercise. Respir. Physiol. Neurobiol. *190*, 142–148.

Weber, W., and Fussenegger, M. (2007). Inducible product gene expression technology tailored to bioprocess engineering. Curr. Opin. Biotechnol. *18*, 399–410.

Weber, W., and Fussenegger, M. (2012). Emerging biomedical applications of synthetic biology. Nat. Rev. Genet. *13*, 21–35.

Weber, W., Rimann, M., Spielmann, M., Keller, B., Daoud-El Baba, M., Aubel, D., Weber, C.C., and Fussenegger, M. (2004). Gas-inducible transgene expression in mammalian cells and mice. Nat. Biotechnol. *22*, 1440–1444.

Weber, W., Schoenmakers, R., Keller, B., Gitzinger, M., Grau, T., Daoud-El Baba, M., Sander, P., and Fussenegger, M. (2008). A synthetic mammalian gene circuit reveals antituberculosis compounds. Proc. Natl. Acad. Sci. USA *105*, 9994–9998.

Wieland, M., and Fussenegger, M. (2012). Reprogrammed cell delivery for personalized medicine. Adv. Drug Deliv. Rev. *64*, 1477–1487.

Wiznerowicz, M., Szulc, J., and Trono, D. (2006). Tuning silence: conditional systems for RNA interference. Nat. Methods *3*, 682–688.

Wurm, F.M. (2004). Production of recombinant protein therapeutics in cultivated mammalian cells. Nat. Biotechnol. *22*, 1393–1398.

Ye, H., Daoud-El Baba, M., Peng, R.W., and Fussenegger, M. (2011). A synthetic optogenetic transcription device enhances blood-glucose homeostasis in mice. Science *332*, 1565–1568.

Young, E.W., and Beebe, D.J. (2010). Fundamentals of microfluidic cell culture in controlled microenvironments. Chem. Soc. Rev. *39*, 1036–1048.